AD-A048 749 NAVAL RESEARCH LAB WASHINGTON D C F/G 20/4
TRANSIENT FREE-SURFACE HYDRODYNAMICS.(U)
NOV 77 M J FRITTS
UNCLASSIFIED NRL-MR-3651 SBIE-AD-E000 071 NL

2 OF 2
AD
A048749

END
DATE
FILMED
7-78
DDC

SUPPLEMENTARY

INFORMATION

AD-A048749

To: Distribution list for NRL Memorandum Report 3651, "Transient Free-Surface Hydrodynamics," by M. J. Fritts, November 1977.

The following changes should be made:

Sponsors statement should be deleted on front cover. On Form 1473, blocks 10 and 18, Project Number should be RR-014-0302.

AD-A048 749 NAVAL RESEARCH LAB WASHINGTON D C F/G 20/4
TRANSIENT FREE-SURFACE HYDRODYNAMICS.(U)
NOV 77 M J FRITTS
UNCLASSIFIED NRL-MR-3651 SBIE-AD-E000 071 NL

1 OF 2
ADA048 749

END
DATE FILMED
2-78
DDC

CONT.

(12) NW

NRL Memorandum Report 3651

Transient Free-Surface Hydrodynamics

M. J. FRITTS

Plasma Dynamics Branch
Plasma Physics Division

November 1977

This report was sponsored by the Office of Naval Research under Contract RR-001-0941

NAVAL RESEARCH LABORATORY
Washington, D.C.

(18) SBIE

(19) AD-E000 071

(14) NRL-MR-3651

SECURITY CLASSIFICATION OF THIS PAGE (When Data Entered)

REPORT DOCUMENTATION PAGE

READ INSTRUCTIONS BEFORE COMPLETING FORM

1. REPORT NUMBER: NRL Memorandum Report 3651
2. GOVT ACCESSION NO.
3. RECIPIENT'S CATALOG NUMBER

(6) 4. TITLE (and Subtitle): TRANSIENT FREE-SURFACE HYDRODYNAMICS.

(9) 5. TYPE OF REPORT & PERIOD COVERED: Interim report on a continuing NRL problem.

6. PERFORMING ORG. REPORT NUMBER

(10) 7. AUTHOR(s): M. J. Fritts

8. CONTRACT OR GRANT NUMBER(s)

9. PERFORMING ORGANIZATION NAME AND ADDRESS: Naval Research Laboratory, Washington, D.C. 20375

10. PROGRAM ELEMENT, PROJECT, TASK AREA & WORK UNIT NUMBERS: NRL Problem H02-39; (17) RR-011-0941; (16) RR011091

11. CONTROLLING OFFICE NAME AND ADDRESS: Office of Naval Research, 800 N. Quincy St., Arlington, VA 22217

(11) 12. REPORT DATE: November 1977

13. NUMBER OF PAGES: 37

14. MONITORING AGENCY NAME & ADDRESS (if different from Controlling Office)

15. SECURITY CLASS. (of this report): UNCLASSIFIED (12) 38 p.

15a. DECLASSIFICATION/DOWNGRADING SCHEDULE

16. DISTRIBUTION STATEMENT (of this Report)

Approved for public release; distribution unlimited.

DDC RECEIVED JAN 19 1978 B

17. DISTRIBUTION STATEMENT (of the abstract entered in Block 20, if different from Report)

6115 3N

18. SUPPLEMENTARY NOTES

This report was sponsored by ONR under Project RR0110941, titled Computational Fluid Dynamics.

19. KEY WORDS (Continue on reverse side if necessary and identify by block number)

Numerical methods
Hydrodynamics
Lagrangian
Triangular grid
Conservation

20. ABSTRACT (Continue on reverse side if necessary and identify by block number)

The control volume approach is used to obtain a finite-difference scheme for a Lagrangian formulation of inviscid incompressible flow using an irregular triangular mesh. The method permits grid reconnections and allows local vertex addition and deletion. Algorithms are presented which conserve divergence, vorticity, mass, momen-

(Continues)

over

DD FORM 1 JAN 73 1473 EDITION OF 1 NOV 65 IS OBSOLETE S/N 0102-014-6601

SECURITY CLASSIFICATION OF THIS PAGE (When Data Entered)

251 950

20. Abstract (Continued)

tum and energy even during grid restructuring. Examples are taken from simulations of shear flow and flow over a hydrofoil in which the restructuring algorithms are crucial. Although the structure of the code is highly scalar, techniques are outlined for producing efficient code even for the new vector computers.

CONTENTS

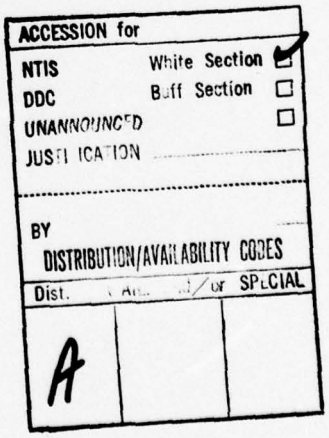

TRANSIENT FREE-SURFACE HYDRODYNAMICS

INTRODUCTION

The hydrodynamics code SPLISH is designed for Lagrangian simulations of transient free-surface phenomena. The present version of the code was developed for inviscid, incompressible flows in two dimensions. The method uses a triangular finite-difference grid in which triangle sides are aligned along free-surfaces, interfaces, boundaries and the perimeters of submerged bodies. The grid internal to these surfaces is left free to reconnect, adjusting to the time-dependent flow.[1,2] In addition, vertices can be added or subtracted as they accumulate or become sparse in convergent and divergent regions of flow. The added flexibility gained through such grid restructuring permits the application of Lagrangian techniques to large classes of problems which were formerly considered solveable only with the aid of diffusive Eulerian rezone methods.[3,4] For example, the simulation of shear flows and flows about obstacles are possible with only local changes in the grid. This paper will present the formulation and the motivation of several such grid restructuring techniques, the algorithms used in implementing them and examples of their use in SPLISH. Because the lack of global ordering in a reconnecting grid is a drawback to its implementation, a discussion of techniques to produce more efficient codes is included. Examples will be given of calculations performed on NRL's TI ASC pipeline computer.

Note: Manuscript submitted November 7, 1977.

THE CONTROL-VOLUME APPROACH

For a Lagrangian formulation of inviscid, incompressible flow, the basic equations are

$$\rho \frac{d\bar{V}}{dt} = - \bar{\nabla} P - \rho g \hat{y} \tag{1}$$

and

$$\bar{\nabla} \cdot \bar{V} = 0 \tag{2}$$

together with the conservation of mass, momentum and energy. There are, of course, many possible ways to design finite-difference schemes for these equations. However, it is in general not possible to determine which approach will be successful.[5] For the case of triangular grids, and in particular reconnecting grids, there does not exist a literature of proven techniques. Therefore the method chosen for SPLISH was the control-volume approach, in which the finite-difference equations are formulated to satisfy the conservation laws macroscopically, over a computational cell. In this way the conservation of physical quantities is explicitly satisfied by the scheme at the outset, and corrections for non-conservation are eliminated.[6,7,8]

The definition of the control volume will of course depend on the location at which physical variables are applied on the grid. It is natural to specify positions and pressures at vertices, since the Lagrangian surfaces coincide with surfaces on which pressure is defined as a boundary condition. In our formulation velocities and densities are triangle centered, yielding a staggered mesh. Pressure gradients are therefore piecewise linear within each triangle and discontinuous at triangle sides, as are the triangle velocities and densities.

Therefore all the variables in Eq. (1) are triangle centered and it is easy to advance the triangle velocities either implicitly or explicitly.

The vertex-centered control volumes, CV, are used to define the new pressures through Eq. (2), expressed as an integral invariant:

$$\int_{CV} \bar{\nabla} \cdot \bar{V} \, dV = 0 \tag{3}$$

That is, the pressures at the vertices are iterated until the resultant triangle velocities reflect a divergence-free condition for each control volume. An obvious construction for a control volume for this application is shown in Figure 1. The vertex-centered control volume is defined by lines extending from the triangle centroids to the triangle side midpoints. This permits a unique, uniform and complete tessalation of the entire computational region. The control volume for each vertex contains exactly one-third of the area of each of the adjacent triangles. Because pressures are defined as boundary conditions, the control volumes are altered near boundaries as shown in Figure 2. In this way the pressures at vertices near the boundaries enforce a divergence-free condition over the additional area as well.

There is another constraint implicit in Eq. (1). Taking the curl of both sides, we have

$$\frac{d(\bar{\nabla} \times \bar{V})}{dt} = - \left(\bar{\nabla} \times \frac{\bar{\nabla} P}{\rho}\right) \tag{4}$$

For homogeneous systems this implies that $\bar{\nabla} \times \bar{V}$ is an invariant for every control volume since $\bar{\nabla} \times \bar{\nabla}P \equiv 0$. With a properly defined $\bar{\nabla}P$, the finite difference formulation also yields $\bar{\nabla} \times \bar{\nabla}P = 0$, so that the vorticity cannot be altered by the pressure gradients alone. However, this invariant does not ensure the conservation of vorticity over a complete timestep by itself. The velocities are triangle-centered, and advancing the vertex positions means altering the size and shape of the control volumes while leaving the velocities unchanged. In other words the integrated region is changed but not the integrand. Therefore the updating of vertex positions dictates an accompanying change in triangle velocities to keep the vorticity conserved. This is shown explicitly in Figure 3. The rotation and stretching of the triangle has necessitated a rotation and diminishing of the triangle velocity such that the $\bar{V} \cdot d\bar{\ell}$ line integral contributions within the triangle for each of the three vertex control volumes remains constant.

Thus far we have shown only that a logical extension of the control volume approach is applicable to a general triangular mesh. It can lead to finite-difference formulations which macroscopically conserve appropriate physical quantities, regardless of how irregular the mesh becomes. The real utility of this approach can be seen, however, when we allow the mesh the freedom to reconnect.

RECONNECTIONS

Despite the assurance that both the curl and divergence can be conserved, solutions through such Lagrangian algorithms can still

yield grossly erroneous results. Figure 4a illustrates a sample calculation of shear flow. Triangles below the center of the fluid are moving to the left with velocity $-\vec{U}$, and those above are moving to the right with velocity $\vec{U}$. The vertices lying directly on the shear interface are stationary, while those above and below move with the triangle velocities. The shear layer is in an unstable equilibrium and should persist until round-off errors accumulate enough to perturb the layer. However, even in the absence of round-off in the positions, the scheme will quickly fail since the triangles on either side of the boundary will become stretched. Very soon pressure gradients will be calculated which involve vertices far removed from each other as shown in Figure 4b. Although the area of each triangle remains constant (and each control volume divergence-free) the convergence of the iterations would slow and truncation errors build rapidly as the triangle sides lengthened. The very appearance of the grid reflects the non-physical situation in which pressures far removed from their co-triangular points on the interface directly influence their behavior, whereas those in the immediate vicinity have little effect.

Clearly, allowing the mesh to reconnect can solve this dilemma. After reconnection the finite-differences will again only involve neighboring vertices. The most obvious criterion for reconnection is based on this premise. Any interior mesh line is associated with a triangle on either side. The line can therefore be viewed as one of two possible diagonals of the quadrilateral formed by these two triangles. One reconnection prescription is to select the shorter of the two diagonals, provided the resulting triangles are not too unequal

in size. This last caveat can be quantified in a number of ways, of course. For example, this algorithm would remove the line from vertex 1 to vertex 3 and subtract a line from vertex 2 to vertex 4 only in Figure 5a. In Figure 5b the new line would lie outside the quadrilateral and in Figure 5c the post-reconnection triangles would be vastly different in size. Thus reconnection should not be performed.

Despite the simplicity and physical motivation of such an algorithm, it is not obvious that it is the preferred one. The expression for a general triangular mesh Poisson equation is[8]

$$\sum_{i\textcircled{c}} \frac{1}{2A_{i+\frac{1}{2}}} \left[\varphi_i\, \hat{z} \times (\bar{r}_c - \bar{r}_{i+1}) + \varphi_{i+1}\, \hat{z} \times (\bar{r}_i - \bar{r}_c) + \varphi_c\, \hat{z} \times (\bar{r}_{i+1} - \bar{r}_i)\right] \times \frac{(\bar{r}_{i+1} - \bar{r}_i)}{2} \cdot \hat{z} = 0 = A_{cv} (\bar{\nabla} \cdot \bar{V})_{cv} \qquad (5)$$

The vertex c is the central vertex as shown in Figure 6a. The $\sum_{i\textcircled{c}}$ is a sum over all triangles adjacent to c and the labelling for the $i + \frac{1}{2}$th triangle is as shown in the figure. $A_{i+\frac{1}{2}}$ is the area of the $i + \frac{1}{2}$th triangle. A_{cv} is the area of the control volume about vertex c and $(\bar{\nabla} \cdot \bar{V})_{cv}$ is the finite difference form of Eq. (3). The coefficient a_c of the φ_c term is

$$a_c = -\sum_{i\textcircled{c}} \frac{|r_{i+1} - r_i|^2}{4A_{i+\frac{1}{2}}} \qquad (6)$$

and is always negative. The coefficient of the φ_i term has contributions from just two triangles $A_{i-\frac{1}{2}}$ and $A_{i+\frac{1}{2}}$, and is

$$a_i = - \frac{(\bar{r}_c - \bar{r}_{i+1}) \cdot (\bar{r}_{i+1} - \bar{r}_i)}{4A_{i+\frac{1}{2}}} - \frac{(\bar{r}_{i-1} - \bar{r}_c) \cdot (\bar{r}_i - \bar{r}_{i-1})}{4A_{i-\frac{1}{2}}} \tag{7}$$

This coefficient reduces to

$$a_i = \tfrac{1}{2}[\cot \theta^- + \cot \theta^+] \tag{8}$$

where θ^+ and θ^- are shown in figure 6b. Since θ^+ and θ^- are both within the range of 0° to 180° (in positive area triangles), then this term is negative only when $\theta^+ + \theta^- > 180^\circ$, since

$$a_i = \frac{\sin(\theta^+ + \theta^-)}{2 \sin\theta^+ \sin\theta^-} \tag{9}$$

Therefore the matrix represented by Eq. (5) is diagonally dominant if $\theta_i^+ + \theta_i^- \leq 180^\circ$ for each i. This provides another uniquely defined reconnection algorithm, since the sum of both such pairs of angles in the quadrilateral is just 360°. Whenever $\theta_i^+ + \theta_i^- > 180^\circ$, the line is reconnected to the opposite diagonal. In other words, we have a reconnection algorithm which automatically ensures the diagonal dominance of the Poisson Equation for an irregular triangular mesh. This algorithm also automatically ensures that a diagonal outside the quadrilateral is never chosen.

Whichever reconnection algorithm is chosen, during a reconnection the smallest physically definable cell is the quadrilateral, and not the triangles. It is reasonable then to ensure that quadrilateral properties are unchanged during a reconnection. In other words, the

quadrilateral becomes a control volume over which certain variables must be conserved. The reconnection is further complicated by its alteration of the vertex control volumes of each of its vertices, as shown in Figure 7. Nevertheless, it would be desirable that the conservation laws enforced through vertex control volumes remain in force during the reconnection. For example, to keep the vorticity and divergence conserved the portions of the integrals $\int_{cv} \bar{\nabla} \cdot \bar{V}\, dV$ and $\int_{surface} \bar{\nabla} \times \bar{V} \cdot d\bar{A}$ within the old and new triangles must be the same before and after the reconnection. Since there are four vertices with two equations for each and only four triangle velocity components to be changed, it would seem that both integrals cannot remain unaltered. In fact the eight equations are not independent. There exists a unique solution for every interior vertex which satisfies both constraints. It is given by

$$\begin{pmatrix} V_{Bx} \\ V_{By} \\ V_{Fx} \\ V_{Fy} \end{pmatrix} = \frac{1}{\bar{R}\cdot\bar{R}} \begin{pmatrix} -\bar{R}\cdot\bar{D} & -2A_F & -\bar{R}\cdot\bar{C} & 2A_F \\ 2A_F & -\bar{R}\cdot\bar{D} & -2A_F & -\bar{R}\cdot\bar{C} \\ \bar{R}\cdot\bar{A} & 2A_B & \bar{R}\cdot\bar{B} & -2A_B \\ -2A_B & \bar{R}\cdot\bar{A} & 2A_B & \bar{R}\cdot\bar{B} \end{pmatrix} \begin{pmatrix} V_{Rx} \\ V_{Ry} \\ V_{Lx} \\ V_{Ly} \end{pmatrix} \quad (10)$$

where the vector definitions of $\bar{A}$, $\bar{B}$, $\bar{C}$, $\bar{D}$ and $\bar{R}$ are given in Figure 8, $\bar{V}_R$ and $\bar{V}_L$ are the triangle velocities before reconnection and $\bar{V}_B$, $\bar{V}_F$ and A_B, A_F are the triangle velocities and areas after the reconnection.

This solution includes a valuable bonus. Not only is it unique, but it is reversible. Re-reconnecting a line yields the original

triangle velocities as well as the original vertex control volume configurations. This is a desirable feature since it mirrors yet another implicit property of the basic equations, time reversibility.

As stated above, Eq. (10) also preserves the quadrilateral velocity. That is

$$A_Q\bar{V}_Q = A_R\bar{V}_R + A_L\bar{V}_L = A_F\bar{V}_F + A_B\bar{V}_B \tag{11}$$

where

$$A_Q = A_R + A_L \equiv A_F + A_B \,, \tag{12}$$

The mass of the quadrilateral is just the sum of the triangle masses, or

$$M_Q = A_R\rho_R + A_L\rho_L = A_F\rho_F + A_B\rho_B \,. \tag{13}$$

Therefore strict mass conservation can also be enforced despite the destruction and creation of triangles by constraining the new densities through Eq. (13). By Eq. (11) and (13) V_Q abd M_Q are both separately conserved, and therefore so is the quadrilateral momentum and kinetic energy. The pressures are defined at vertices whose positions do not change during reconnection, and the potential energy can be altered only by the different definitions of $\frac{\bar{\nabla}P}{\rho}$. Since we are free to choose both new densities, and have only one equation, Eq. (13), to satisfy, we also control the change in potential energy through Equation (4), which provides the second density constraint. This specifies that the amount

of vorticity generated within the quadrilateral is the same before and after the reconnection.

Reconnections then offer a very attractive alternative to global rezoning. The control volume approach leads to algorithms which conserve vorticity and divergence in the control volume about each vertex despite the reconnections. The algorithms also conserve mass, energy and momentum on the basis of triangular and quadrilateral control volumes and further exhibit time reversibility. Finally, the prescription for the occurrence of reconnections can be chosen to preserve ordering by nearest neighbors or to preserve the diagonal dominance of Poisson's equation over the irregular grid.

These routines have been tested on the problem of shear layer instability.[7] Figure 9 illustrates a simulation in which the initial shear layer was not perturbed. The grid has not changed although each vertex in the upper half of the fluid has traversed the entire grid ten times. Figure 10 shows the grid and a marker particle display for the case of an initial perturbation which has grown to a Kelvin-Helmholtz billow (top row), and after the mature billow begins to shear. The calculation agrees well with the predicted growth rates. Only the reconnection algorithms were used in restructuring the grid, and the grid at t = .329 sec. exhibits two irregularities. Two of the vertices have become too close, forming thin elongated triangles, and a third vertex has become enclosed within a triangle. Other grid restructuring is clearly needed. These additional techniques will be discussed in the following section.

VERTEX ADDITION AND DELETION

The fluid flow near a separatrix is another area in which traditional numerical Lagrangian treatments fail. Figure 11 illustrates a sample grid for a submerged hydrofoil near a free surface. The flow is directed to the right initially with velocity $\vec{U}$. Clearly as the flow develops vertices will tend to accumulate at the forward stagnation point. At the same time the vertices on the hydrofoil will move with the flow along the hydrofoil and accumulate (by pairs) in its wake. After a very short time the gridding will deteriorate to a denser grid before and after the hydrofoil and a sparse grid along the hydrofoil itself.

These problems do not derive from an ill-chosen initial grid but are inherent in Lagrangian treatments. By choosing the mid-line of the hydrofoil between an initial row of vertices, a situation develops in which vertices of the same triangle flow toward opposite sides of the obstacle, leading to a nonsensical calculation of fluid pressure gradients between vertices separated by an obstacle. Fixing the vertices on the hydrofoil surface and allowing reconnections is neither physically desirable nor effective. A tangled grid results from inverted triangles forming over the hydrofoil. The advantage of the present treatment using a control volume formulation is that while these problems are difficult, they are still soluble.

The problem of representing flow near separatrices could be resolved if it were possible to add and subtract vertices from the calculation as needed without altering the physically conserved properties of the flow. Fortunately, such schemes are possible, and may be derived

in the same spirit as the reconnection algorithm by using a control volume approach. For example, the simplest way to add a vertex to the fluid is at the centroid of a triangle. Lines are drawn from the new vertex to each of the existing vertices, leaving three new triangles in place of the old one. If all triangle variables are chosen to be identical with the original variables of the old triangle, the behavior of the three triangles clearly does not alter the fluid motion since it is identical to that of the initial triangle. If the vertex pressure is chosen as the average of the three vertex pressures, we have likewise left unaffected the pressure gradients throughout the area occupied by the old triangle. In other words, the three new triangles behave exactly as the former one, and are indistinguishable from it since the vertex remains enclosed within its former boundaries. However, we know that the reconnection algorithm will eventually alter one of the triangle sides if a vertex in the vicinity of the old triangle was really needed. Otherwise the new vertex will continue to behave as if it were not there. But the reconnection is also conservative as shown above, and once a reconnection occurs we have successfully introduced a vertex while maintaining strict conservation of flow properties.

The converse is also true. If a vertex becomes enclosed in a triangle, the behavior of that triangle is not altered if the vertex is removed and the new larger triangle given the velocity

$$A_4\bar{V}_4 = A_1\bar{V}_1 + A_2\bar{V}_2 + A_3\bar{V}_3 \qquad (14)$$

where triangle 4 encompasses the three triangles 1, 2 and 3. Since the mass of the resultant triangle can be defined in a similar manner, the momentum of the larger triangle has not been altered. Therefore for both addition and subtraction of vertices, the larger triangle acts as a control volume in exactly the same sense as the quadrilateral for the reconnections. What has been lost is the information about the behavior of the pressure gradients and velocity gradients within the triangle. This information has been averaged out and replaced by a linear variation across the triangle. All we have suffered is a loss in resolution, exactly what we set out to do in removing the vertex.

This claim requires elaboration. The removal of a vertex implies the alteration of four vertex control volumes, one of which is removed, and such a drastic change does not seem consistent with a mere change in resolution. Figure 12 illustrates the triangles before and after vertex removal. Before the vertex is deleted the relevant contribution to the vorticity integrals about each vertex are

$$\int_1 \bar{V} \cdot d\bar{\ell} = \vec{V}_i \cdot \frac{(\bar{r}_4 - \bar{r}_2)}{2} + \vec{V}_k \cdot \frac{(\bar{r}_3 - \bar{r}_4)}{2} = \xi_1$$

$$\int_2 \bar{V} \cdot d\bar{\ell} = \vec{V}_j \cdot \frac{(\bar{r}_4 - \bar{r}_3)}{2} + \vec{V}_i \cdot \frac{(\bar{r}_1 - \bar{r}_4)}{2} = \xi_2$$

$$\int_3 \bar{V} \cdot d\bar{\ell} = \bar{V}_k \cdot \frac{(\bar{r}_4 - \bar{r}_1)}{2} + \bar{V}_j \cdot \frac{(\bar{r}_2 - \bar{r}_4)}{2} = \xi_3$$

$$\int_4 \bar{V} \cdot d\bar{\ell} = \bar{V}_i \cdot \frac{(\bar{r}_2 - \bar{r}_1)}{2} + \bar{V}_j \cdot \frac{(\bar{r}_3 - \bar{r}_2)}{2} + \bar{V}_k \cdot \frac{(\bar{r}_1 - \bar{r}_3)}{2} = \xi_4 \qquad (15)$$

After vertex 4 is eliminated its vorticity must be apportioned to vertices 1 through 3 in some manner;

$$\int_1 \bar{V} \cdot d\bar{\ell} = \bar{V}_\ell \cdot \frac{(\bar{r}_3 - \bar{r}_2)}{2} = \xi_1 + \xi_1'$$

$$\int_2 \bar{V} \cdot d\bar{\ell} = \bar{V}_\ell \cdot \frac{(\bar{r}_1 - \bar{r}_3)}{2} = \xi_2 + \xi_2'$$

$$\int_3 \bar{V} \cdot d\bar{\ell} = \bar{V}_\ell \cdot \frac{(\bar{r}_2 - \bar{r}_1)}{2} = \xi_3 + \xi_3'$$

and $$\xi_1' + \xi_2' + \xi_3' \equiv \xi_4 \tag{16}$$

Eliminating ξ_1, ξ_2 and ξ_3 between Eq. (15) and (16), we have

$$\bar{V}_i \cdot (\bar{r}_4 - \bar{r}_2) + \bar{V}_k \cdot (\bar{r}_3 - \bar{r}_4) = \bar{V}_\ell \cdot (\bar{r}_3 - \bar{r}_2) - 2\xi_1'$$

$$\bar{V}_j \cdot (\bar{r}_4 - \bar{r}_3) + \bar{V}_i \cdot (\bar{r}_1 - \bar{r}_4) = \bar{V}_\ell \cdot (\bar{r}_1 - \bar{r}_3) - 2\xi_2'$$

$$\bar{V}_k \cdot (\bar{r}_4 - \bar{r}_1) + \bar{V}_j \cdot (\bar{r}_2 - \bar{r}_4) = \bar{V}_\ell \cdot (\bar{r}_2 - \bar{r}_1) - 2\xi_3' \tag{17}$$

Substituting $A_\ell \bar{V}_\ell = A_i \bar{V}_i + A_j \bar{V}_j + A_k \bar{V}_k$ into Eq. (17) yields, after some algebra,

$$\xi_1' = A_j \, \xi_4 / A_\ell$$

$$\xi_2' = A_k \, \xi_4 / A_\ell$$

$$\xi_3' = A_i \, \xi_4 / A_\ell$$

where $\xi_1' + \xi_2' + \xi_3' = \xi_4$ since $A_i + A_j + A_k \equiv A_\ell$. Therefore, conserving momentum exactly over the large triangle yields exactly the conservation of vorticity within the affected vertex control volumes. The vorticity carried by the expunged vertex is apportioned by area to the neighboring vertices. If the deleted vertex lies close to one of the remaining vertices, that vertex will carry most of the reassigned vorticity. Therefore the total vorticity is accounted for in a reasonable and natural manner, and momentum is still conserved. Since a similar argument holds for the divergence equations, conservation of flow variables is demonstrated, and a loss in resolution is the only effect.

For the case of an added vertex, the vertex control volume integrals are trivially left unchanged, and the added vertex initially carries no vorticity. Vorticity can accumulate about the added vertex only through reconnections with triangles having dissimilar ρ. That is, vorticity is generated only by density gradients, as expected.

Therefore vertices can be added and subtracted within triangles while conserving flow properties exactly. In both cases the usefulness of this result derive from the reconnection algorithm. Used in tandem with addition and deletion within triangles it provides a general algorthm for altering the grid without disturbing the fluid flow. It has already been shown that reconnection used after addition of a vertex at the triangle centroid liberates the vertex in a conservative manner and

permits it to behave no longer as the centroid of the triangle. The process can also be reversed. The reconnection algorithm can be used to isolate any vertex within a larger triangle. Once this is accomplished the vertex can be averaged out.

The utility of this technique is not limited to interior mesh points. Figure 13a illustrates a triangle at the leading edge of a submerged body. The flow is forcing the triangle vertices on the boundary in opposite directions, and resolution of the leading portion of the hydrofoil is being lost. A point may be added along the body as in 13b. The result may be viewed as the addition of a point within a triangle, but one in which only two of the three smaller triangles survive.

Figure 14a illustrates the reverse situation at the rear of the hydrofoil. There a new line is drawn to enclose the unwanted vertex in a triangle. In Figure 14b the vertex has been removed from the body, leaving the way clear to add a vertex in the fluid, if needed to preserve resolution, as in Figure 14c.

The use of the control volume approach has therefore made possible the dynamic addition and subtraction of vertices exactly where desired and in a fashion which locally and globally conserves the properties of the fluid flow. The combined use of local resolution alteration and reconnection algorithms permits Lagrangian calculations of extremely complicated flows.

EFFICIENCY

It is obvious that for a code such as SPLISH any global ordering of the grid would soon be invalidated by reconnections and by the

addition and deletion of vertices. Since standard fast Poisson solvers rely on such an implicit ordering among vertices, it is appropriate to conclude this paper with some remarks on its efficiency.

The new generation of vector computers provides a good starting point for such a discussion. The increased speed of these computers is attained in large part by their ability to perform quickly a given operation on large numbers of members of an array, which are preferably stored contiguously in memory. Calculations on a vector computer are therefore performed operation by operation for all array members instead of performing the whole sequence of operations in turn for each member of an array. The ordering of the vertices becomes all importnat, and a highly disordered code such as SPLISH is almost totally unsuitable for efficient operation. However, despite such obvious problems, the entire SPLISH code has been optimized for the NRL TI ASC vector computer.

Our first example is the reconnection algorithm itself. The heart of the reconnection algorithm is based on the quadrilateral about the line. However, every reconnection that is performed redefines the quadrilaterals for each of the four lines which make up the original quadrilateral. This situation is highly scalar, in that a single reconnection may invalidate the possible reconnection of four neighboring lines. Therefore it is impossible to allow reconnections to proceed in parallel, and the complete calculation for one must be performed before the next is initiated.

However, even in this situation some increase in speed may be gained through efficient coding. Clearly a good deal of the time in the reconnection algorithm is spent in testing each line for a possible

reconnection. In general, very few of the lines reconnect for a given timestep. The flow is following local streamlines. Therefore the test can be vectorized provided its output is a list of lines which may want to be reconnected. Each of these (few) lines is then passed through the scalar reconnect routines, in which they are retested and the reconnection performed if it is still desirable. An iteration through this procedure may be desired, but in most cases is not necessary since most reconnections occur remote from each other. In no realistic case tested were more than three iterations required to reach the final grid.

The savings in computer time of course depends on the number of lines reconnected. For roughly one percent of the lines reconnecting per timestep (an average case), the vectorized test followed by scalar reconnect is ten times faster. The same is true of all the grid restructuring algorithms. Large saving in time can accrue through vectorizing the tests which must be performed on every line or triangle. The grid alterations must remain scalar, but are relatively few in number.

The second example is the solution of Poisson's Equation. In SPLISH the pressures are adjusted at each vertex iteratively to enforce a divergence-free condition for each vertex control volume. As shown by Eq. (5), coefficients of each term are expressed in terms of the positions of co-triangular vertices. Since there is no global ordering, such a calculation accesses storage almost randomly. That is, the code is highly scalar, and its efficiency on a vector machine is correspondingly poor.

Nevertheless, it is also possible to obtain vectorized code in this situation. The solution is to precompute arrays which duplicate

the position data for each neighboring vertex. These "alias" arrays can be ordered consecutively in core in exactly the ordering necessary for efficient vectorized code. Therefore although a good deal of extra scalar computation is performed, the increase in speed obtainable for the vectorized code more than compensates for the extra time. The use of "alias" arrays has yielded decreases in computation time of roughly a factor of three. Typical timings for the Poisson solver are now 6.8 milliseconds per iteration for 120 vertices or about 60 microseconds per iteration per vertex.

Although such increases in speed are encouraging, they are not the final solution. Large calculations will require faster solvers. The most promising approach is through the use of direct solvers, rather than iterative ones. Although the matrix representing Eq. (5) does not exhibit the ordering of rectangular meshes, it is nonetheless sparse. Furthermore, if the vertices are preordered by position, the non-zero members will lie along rather diffuse bands. Recently, there has been an increase in interest in fast solvers for such banded matrices and several techniques look particularly encouraging.[9,10] The outlook is very good. Not only is a large class of problems now amenable to Lagrangian calculations, but also at a computational cost per zone competitive with other techniques.

References

1. J. P. Boris, M. J. Fritts and K. L. Hain, "Free Surface Hydrodynamics Using a Lagrangian Triangular Mesh." Proceedings of the First International Conference on Ship Hydrodynamics, Oct. 20, 1975.

2. W. P. Crowley, "Flag: A Free Lagrange Method," Proceedings of the Second International Conference on Numerical Methods in Fluid Dynamics, Lecture Notes in Physics, Springer-Verlag, New York, 1971.

3. R. K. -C Chan, "A Generalized Arbitrary Lagrangian-Eulerian (Gale) Method for Incompressible Flows with Sharp Interfaces," SAI-73-575-LJ, Nov. 1973.

4. C. W. Hirt, "An Arbitrary Lagrangian-Eulerian Computing Technique," Proceedings of the Second International Conference on Numerical Methods in Fluid Dynamics, Lecture Notes in Physics, Springer-Verlag, New York, 1971.

5. P. J. Roache, Computational Fluid Dynamics, Hermosa Publishers, Albuquerque, New Mexico, 1972, p. 25.

6. M. J. Fritts, "A Numerical Study of Free-Surface Waves," SAI-76-528-WA, Mar. 1976.

7. M. J. Fritts, "Lagrangian Simulations of the Kelvin-Helmholtz Instability, SAI-76-632-WA, Sep. 1976.

8. M. J. Fritts and J. P. Boris, "Solution of Transient Problems in Free Surface Hydrodynamics," NRL Memorandum Report 3446, Feb. 1977.

9. D. S. Kershaw, Private Communication.

10. N. K. Winsor, NRL Memorandum Report 3481, Jun. 1977, to be published in Nuclear Science and Engineering.

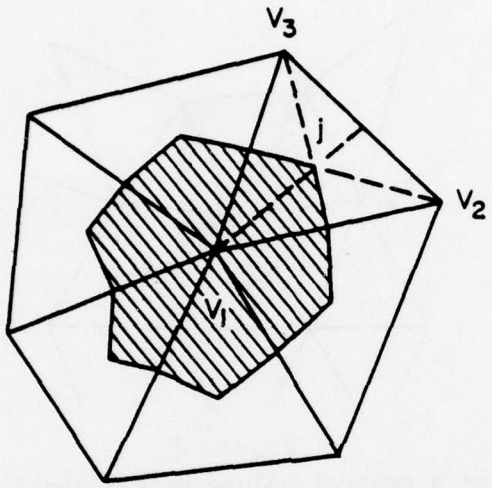

Figure 1

Definition of a control volume about an interior vertex, V_1. The area of triangle j is apportioned equally to the control volumes about V_1, V_2 and V_3.

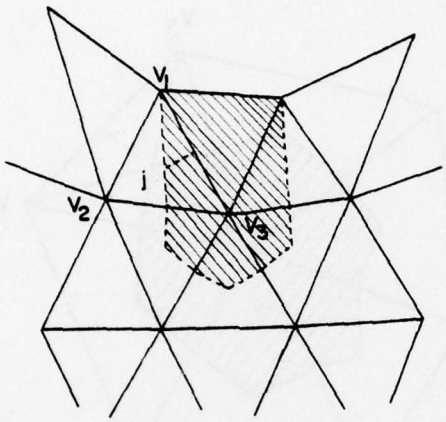

Figure 2

Alteration of a control volume near a boundary. The portion of triangle j normally assigned to the vertex V_1 is divided between vertices V_2 and V_3.

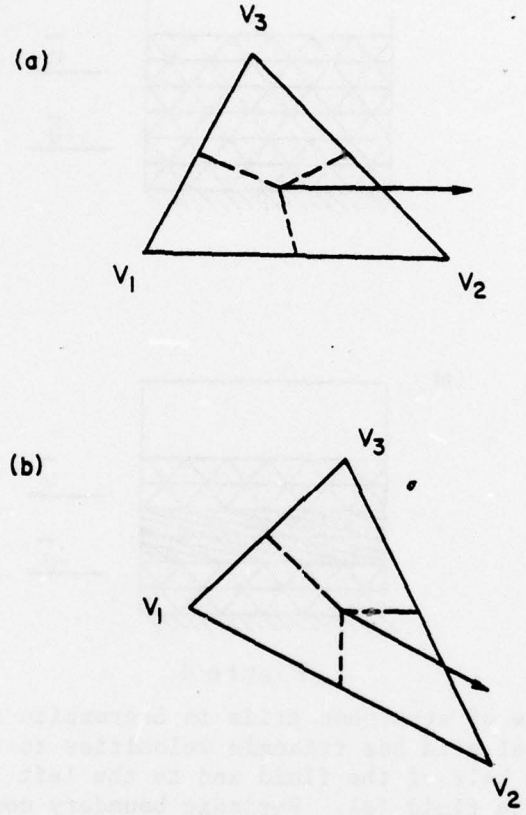

Figure 3

Conservation of vorticity while advancing vertex positions. The triangle velocity is altered such that the $\bar{V}.d\bar{\ell}$ line integral contributions within the rotated and stretched triangle remain the same for each vertex.

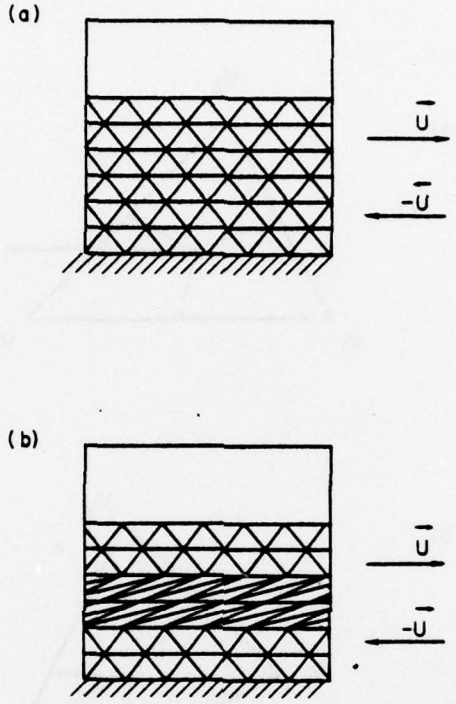

Figure 4

An example of stretched grids in Lagrangian simulations. The initial grid has triangle velocities to the right in the upper half of the fluid and to the left in the lower half of the fluid (a). Periodic boundary conditions are specified on the sides of the region. The grid very quickly distorts in the vicinity of the shear layer (b).

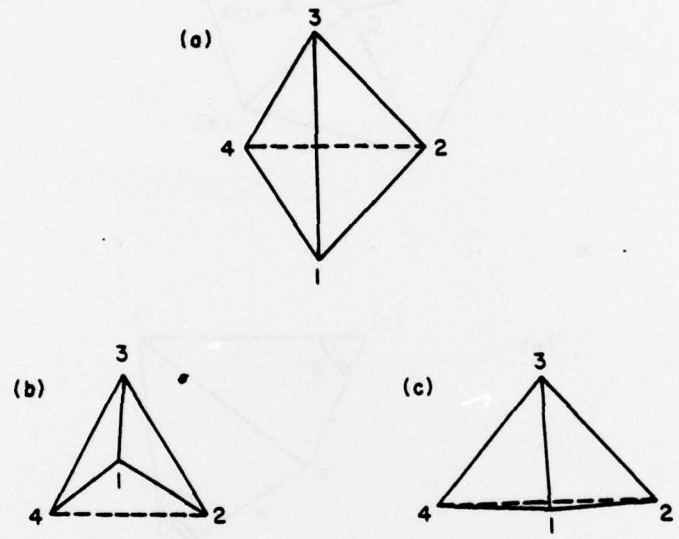

Figure 5

The "nearest neighbor" reconnection algorithm. Lines are reconnected to choose the shortest diagonal of a quadrilateral (a). Lines are not reconnected for "inverted" quadrilaterals even if the exterior diagonal is shorter (b). Nor is the reconnection performed if the resultant triangles are too dissimilar in size (c).

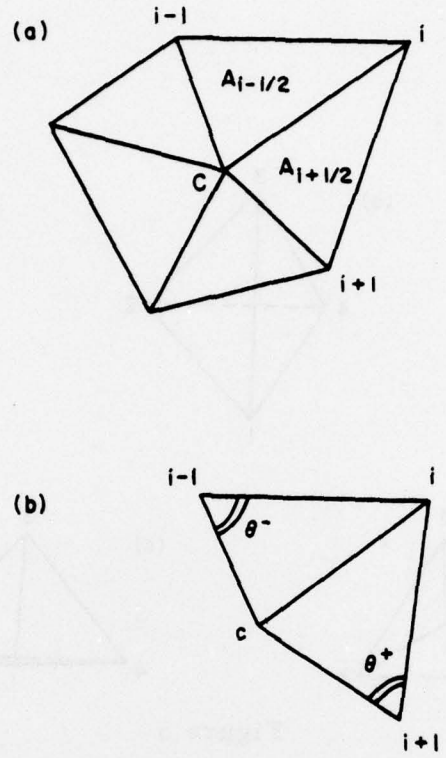

Figure 6

The reconnection algorithm to preserve diagonal dominance of the Poisson Equation. The triangle and vertex labelling used in the Poisson Equation is shown in (a). Figure (b) indicates the angles θ^+ and θ^- used in the reconnection test for the line from vertex c to vertex i.

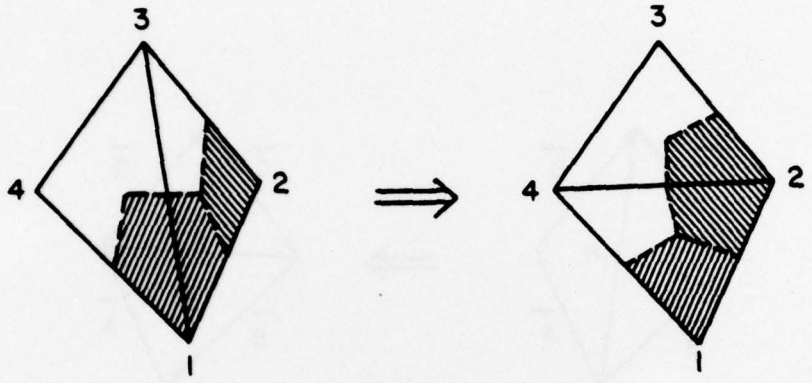

Figure 7

The alteration of control volumes by a reconnection. Portions of the control volumes about vertex 1 and vertex 2 are shown before and after the reconnection.

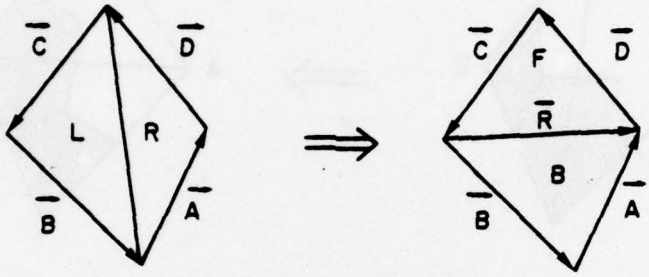

Figure 8.

The labelling for triangles and side vectors used in the reversible algorithm to determine new triangle velocities.

SHEAR FLOW WITH NO PERTURBATIONS

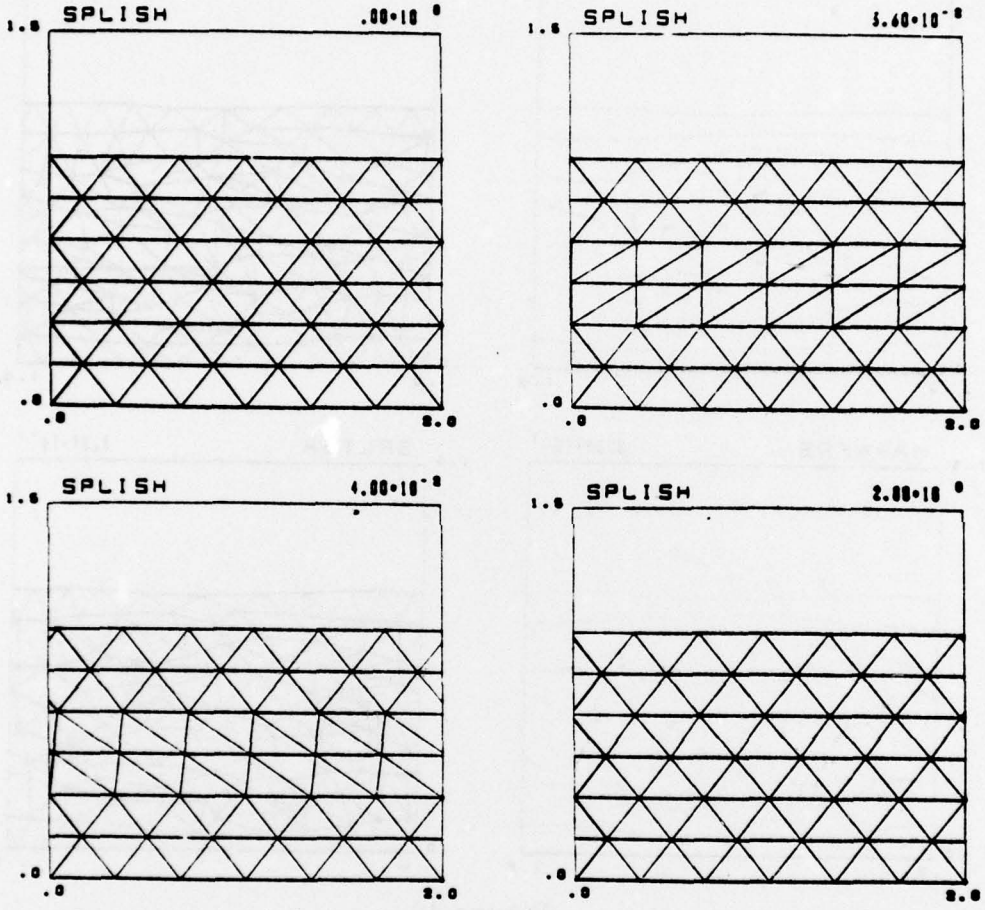

Figure 9

A test of the reconnection algorithm in SPLISH. The grid at various times is presented for a simulation of an unperturbed shear layer. The grid at t = 0 corresponds to that in Figure 4a. However, here the grid reconnects as it stretches, as shown between t = .036 sec and t = .040 sec. In this simulation δt = .004 sec, $|\vec{U}|$ = 5 cm/sec and the length of the system is 2 cm. At t = 2.00 sec each vertex in the upper layer has passed each vertex in the lower layer ten times. Any errors in assignment of triangle velocities would have perturbed the unstable equilibrium of the layer.

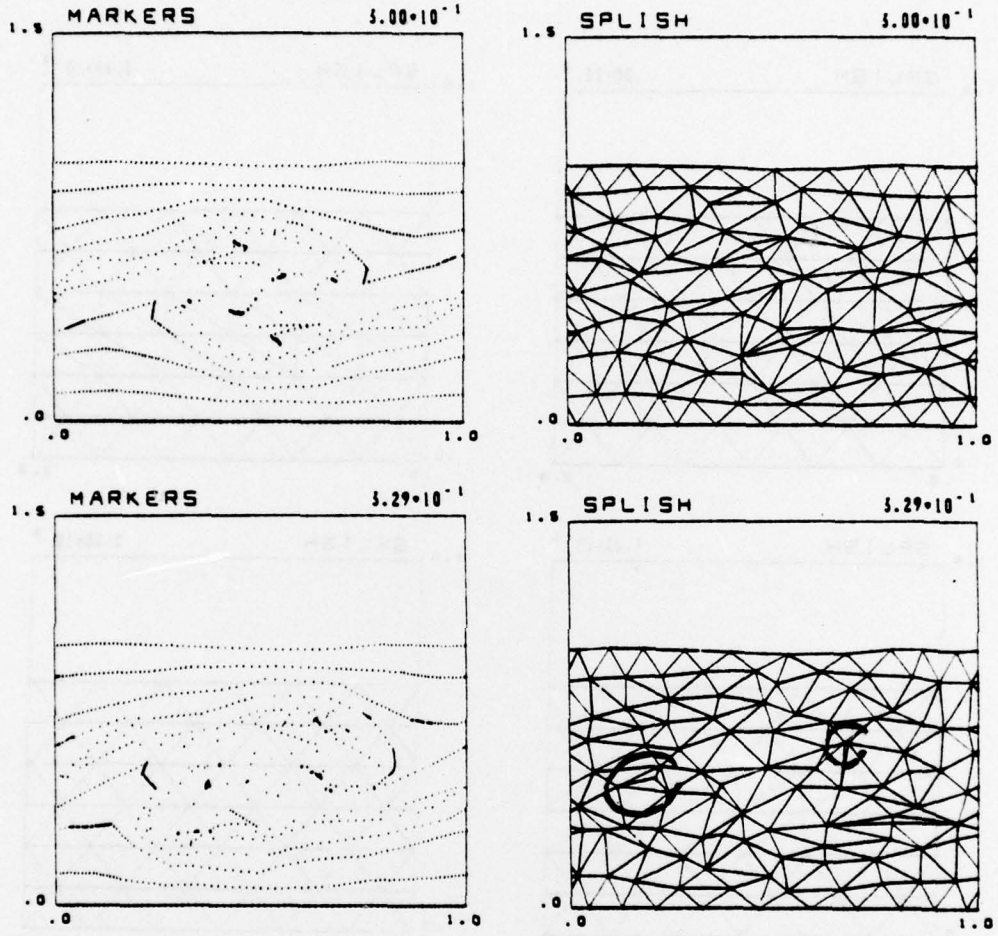

Figure 10

The grid and marker particles at two times in a simulation of a perturbed shear layer. Here δt = .001 sec, $|\vec{U}|$ = 5 cm/sec and the length of the system is 1 cm. At t = .300 sec the perturbed layer has grown to a mature Kelvin-Helmholtz billow. Only reconnections were used in restructuring the grid. At t = .329 sec the billow is shearing. Two grid anomalies are circled.

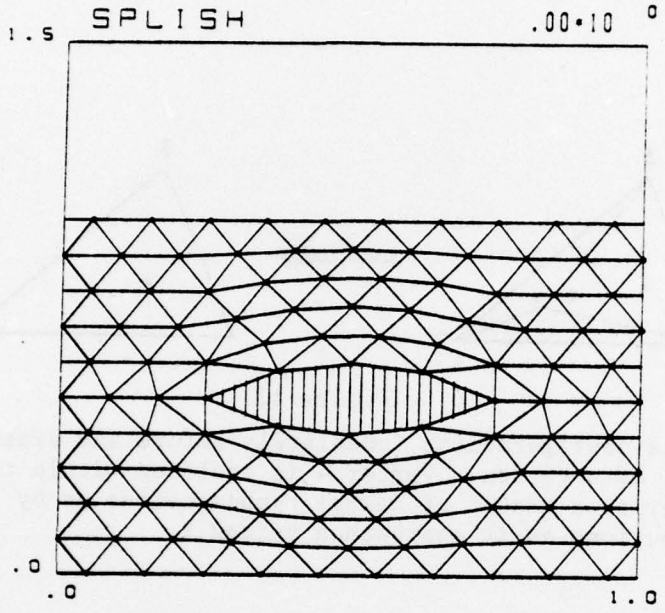

Figure 11

The grid for a hydrofoil near a free surface. The flow is initially directed to the right with velocity $\vec{U}$.

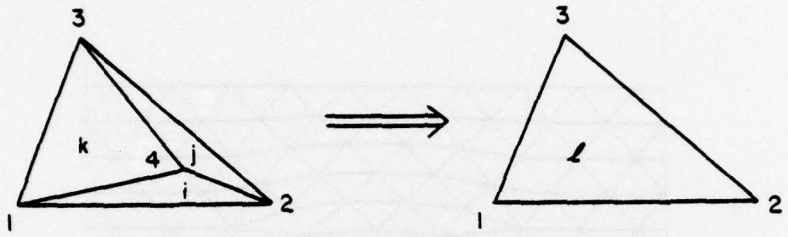

Figure 12

Triangle configurations immediately before and after the removal of a vertex. Vertex 4 is enclosed within triangle ℓ either as a result of normal reconnections or by forcing reconnections as it approaches vertex 2.

Figure 13

The addition of a vertex at a boundary. The vertices on the boundary are moving along opposite sides of a submerged body (a), and resolution is lost for the leading edge of the body. In (b) a new vertex is added on the boundary. The old triangle is deleted and two new triangles are added.

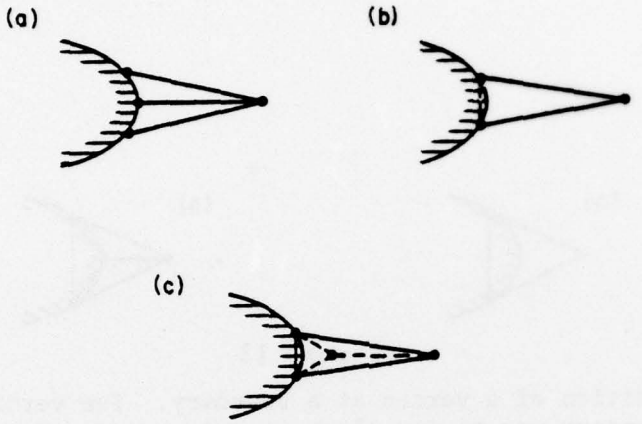

Figure 14

The deletion of a boundary vertex. The flow is converging at the trailing edge of a submerged body (a), resulting in a clustering of vertices and the formation of long thin triangles. In (b) a vertex is removed by drawing a new line to form the enclosing triangle. In (c) a new vertex is added within the elongated triangle to preserve resolution of the flow at the trailing edge. Subsequent reconnections will remove the thin triangles.